Design of a High Mobile Micro Rover within a Dual Rover Configuration for Autonomous Operations

Roland U. Sonsalla[1], Yashodhan Nevatia[2], Martin Fritsche[1],
Joel Bessekon Akpo[1], Jeremi Gancet[2] and Frank Kirchner[1,3]

[1] DFKI Robotics Innovation Center, Bremen, Germany
e-mail: *firstname.lastname@dfki.de*

[2] Space Application Services, Zaventem, Belgium
e-mail: *firstname.lastname@spaceapplications.com*

[3] University of Bremen, Robotics Lab, Bremen, Germany

Abstract

The importance for small and lightweight rovers providing high mobility and versatility in future exploration missions is increasing. Within this paper the terrestrial test platform Coyote II is presented. The rover is equipped with a novel locomotion concept combining hybrid legged-wheels with spherical helical wheels. This allows to perform side-to-side steering movements and yields high mobility performance in rough terrain as well as on soft soils as shown during various laboratory and real environment tests. The rover is specially designed to act as a scout rover paired up with a primary rover for autonomous long term exploration. The operational concept for the scout rover within the two rover team is addressed with respect to the primary rover.

1 Introduction

As opposed to the present extra-terrestrial exploration missions, future mission concepts ask for fast and safe long range traversal through varied expanses of terrain. The main objective of the FASTER EU FP7 project is to improve the mission safety and the effective traverse speed for planetary rover exploration by autonomously determining the traversability of the terrain and lowering the risk of entering hazardous areas. To achieve this goal, it is proposed to introduce a small scout rover accompanying the primary exploration rover. While both, the primary rover and the scout rover are equipped with their own sensor systems, the scout rover is used to scout the terrain ahead of the primary rover to allow fast and safe traversal. For requirements definition and system development, a reference mission scenario similar to the proposed ESA/NASA Mars Sample Return (MSR) mission has been defined, as outlined in [5].

The paper focuses on the mechanical design and evaluation of the Coyote II rover, acting as locomotion test platform for the envisaged scout rover (cf. Figure 1). The general system design of Coyote II is presented, addressing the core functionality and subsystems of the rover. A closer look is given to the overall mechanical construction and the locomotion concept. The rover development is based on a concept study given in [9]. A set of mobility tests, comparing different wheel combinations in terms of mobility and maneuverability is presented, showing the high mobility performance of the rover.

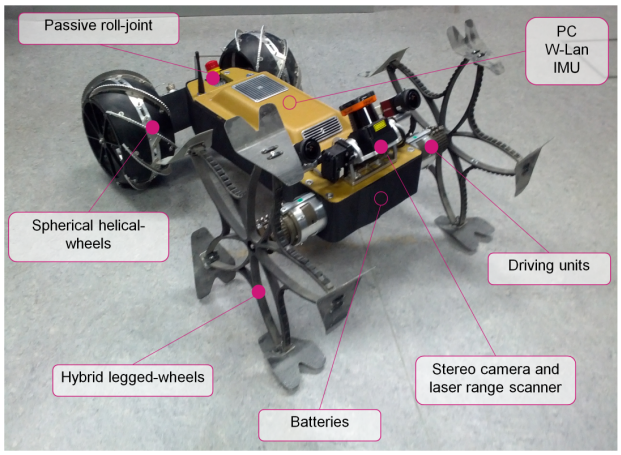

Figure 1. Functional chart of the fully integrated rover platform Coyote II, heighlighting the rover's main elements

Furthermore, the software architecture of the two rover team is outlined. This includes first, the autonomy modules needed on the scout rover and second, the overall integration of the scout rover into the primary rovers software architecture to allow autonomous dual rover operations.

2 System Design

The general design considerations for the scout rover are based on the mission and operation scenario as described in [9]. As the scout rover is considered an additional payload within a robotic exploration mission, its mass and dimensions need to be reduced to a minimum. At the same time, the scout rover needs high mobility and versatility to perform scouting tasks without disturbing the primary rover's traversal and/or mission.

The Coyote II platform as shown in Figure 1 was developed as terrestrial testbed aiming to provide a test platform for software and locomotion tests. The rover embodies five main subsystems, namely: structure and mechanisms, on board data handling (OBDH), communications (COM), electrical power supply (EPS) and navigation sensors. A general overview of these subsystems is given in Table 1 providing the core characteristics of each subsystem.

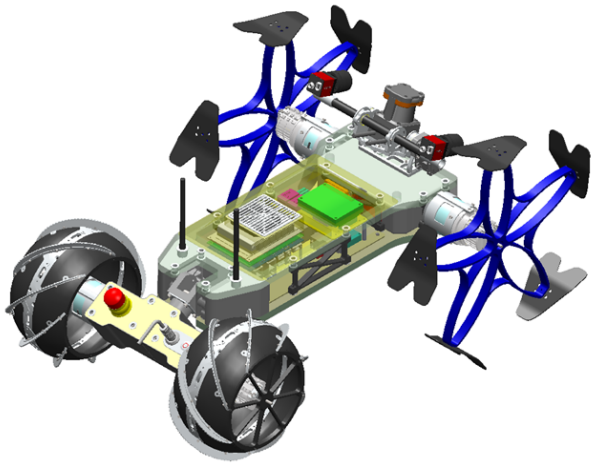

Figure 2. CAD rendering showing the main structure and interior of Coyote II

Table 1. Coyote II: Subsystems Overview

Mechanical Parameter	
Boundary Box	850 × 580 × 410 mm
System Mass	9.2 kg
Wheel torque (max.)	28 Nm
Whell speed (max.)	50 rpm
Front leg length	185 mm
Rear wheel	ø250 mm (incl. 20 mm grousser)
On Board Data Hanlding	
On Board Computer	ComExpress based PC, IntelCore i7-3517UE, 1.7GHz
Communications	
W-Lan Router	2.4 GHz; 802.11n up to 150 Mbits
Remote Control	Bluetooth
Electrical Power Supply	
Primary Battery	LiPo: 44.4 V; 2.1 Ah
Bus Voltages	48 V; 12 V; 5 V
Average power	75 W (straight driving)
Navigation Sensors	
Stereo Camera	AVT F33B (656 × 494 px); FoV: 118.6° (horizontal)
Laser Range Finder	Hokuyo UTM-30XL; 905 nm 270° semicircular FoV
IMU	Xsens MTi-300 AHRS

The relatively low mass of 9.2 kg is achieved by using composite sandwich sheets. The main body of Coyote II is designed like a double-decker structure (cf. Figure 2). The top and bottom layers of the body consist of sandwich sheets with a 12 mm Arix core and 0.5 mm aramid fiber layers, providing a stiff and lightweight structure.

Each wheel is driven by a powerful motor unit including the motor control electronics and a Robodrive ILM 50×8 brushless dc motor in combination with a harmonic drive gear. The motor modules were initially developed for the six-legged walking robot SpaceClimber (cf. [1]) and have proven their robustness.

The remaining elements for OBDH, COM, EPS, and the IMU are integrated within the front body of the rover. A tiltable sensor head is mounted on top of the main body. It is equipped with two wide angle cameras within a stereo camera set-up and a laser range finder for navigation purposes.

The rovers chassis contains a passive roll joint which connects the rover's rear axis to the main body. This allows ground contact of all four wheels even in rough terrain. An additional adjustable hinge joint at the main body allows to manually tilt and fix/lock the rear axis with respect to the rover's front (cf. Figure 2). This joint has specifically been implemented for locomotion test purposes. Shifting the front and rear axis on the same level allows to reconfigure the Coyote II rover into an Asguard-like configuration (cf. [2]) by mounting wheels with the same diameter in the front and in the back.

3 Locomotion Concept

The locomotion concept for Coyote II is inspired by the Asguard and the CESAR rovers (cf. [2] and [8]). Asguard makes use of four hybrid legged-wheels equipped with small rubber feed. The CESAR rover has two hybrid legged-wheels in the front, each leg equipped with wide flat feed, and a paddled drum in the rear. Both rover use skid steering as illustrated in Figure 3(a). The skid steering causes heavy soil disturbances especially in soft soils due to the sideways motions of the wheels. This was identified as a potential issue for the following primary

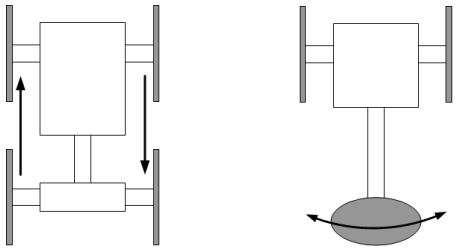

(a) (b)

Figure 3. Steering concepts; (a) skid steering, (b) side-to-side steering

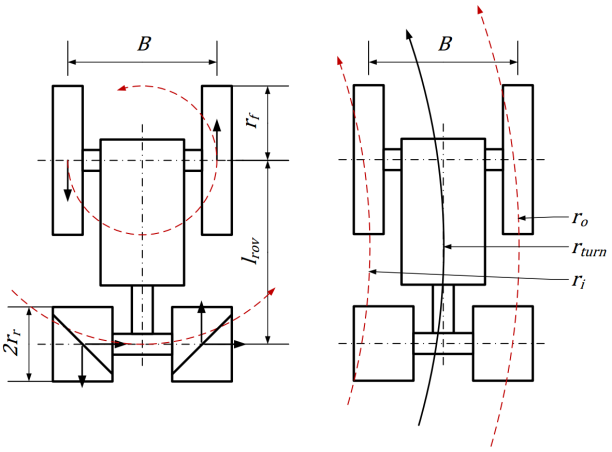

(a) Side-to-side steering kinematics (b) Continuous steering kinematics

Figure 4. Steering kinematics for side-to-side steering and continuous steering maneuvers

rover, which should not face any newly created obstacles by scout rover steering.

In order to reduce the level of soil disturbance due to skid steering, a new locomotion concept was developed for the Coyote II rover. This concept combines the high mobility performance of hybrid legged-wheels with the smooth wheel movement of spherical helical wheels. Applying two helical wheels on the rear axis allows to perform side-to-side steering movements, as shown schematically in Figure 3(b). For steering purposes the helical wheels are able to gain sideways motions, which allows to shift the point of rotation on the front axis. In this case the front wheels can move in their designated direction, which reduces the soil disturbance drastically.

3.1 Steering kinematics

Applying hybrid legged-wheels in the front and helical wheels on the rear axis requires to adapt the wheel rotation speed for the different driving maneuvers. The distance covered by each wheel type can be calculated for the five-legged front wheels according to equation 1 and 2 respectively for the helical rear wheels. The parameter r_f and r_r are representing the leg length and the mean rear wheel radius.

$$D_f = 5\frac{10 \cdot r_f}{\sqrt{50 + 10\sqrt{5}}} \quad (1)$$

$$D_r = 2\pi r_r \quad (2)$$

The dependency of required motor speeds for driving straight is then given by equation 3; with ω_r as rear axle turn rate and ω_f as front axle rotation.

$$F = \frac{D_f}{D_r} = \frac{\omega_r}{\omega_f} \quad (3)$$

The point of rotation is at the center point between the two axles for common skid steering. For side-to-side steering it is intended to shift the point of rotation on the center point of the front axis. This can be achieved due to the sidewards motion of the spherical wheels as shown in Figure 4(a). In this case, the front and rear wheels are following different trajectories.

The distance which is covered in sidewards motion by the helical wheels is dependent on the grousser pitch angle α_g. The helix lead per rotation h_r is calculated by equation 4 while the circumferences of front and rear wheel trajectories are calculated by equation 5 and 6 respectively.

$$h_r = \frac{2\pi r_r}{\tan \alpha_g} \quad (4)$$

$$C_f = \pi B \quad (5)$$

$$C_r = 2\pi l_{rov} \quad (6)$$

Based on the wheel trajectories C_f and C_r and the distance covered per rotation D_f and h_r the turn rates of the front and rear wheels $\omega_{f,\,sts}$ and $\omega_{r,\,sts}$ can be calculated following equation 7 and 8 for side-to-side steering motions.

$$\omega_{f,\,sts} = \frac{C_f}{D_f} \quad (7)$$

$$\omega_{r,\,sts} = \frac{C_r}{h_r} \quad (8)$$

This yields the motor speed ratio F_{sts} for performing side-to-side steering movements as given in equation 9.

$$F_{sts} = \frac{\omega_{r,\,sts}}{\omega_{f\,sts}} \quad (9)$$

The following parameter are given for Coyote II: front wheel leg length $r_f = 185$ mm, front track width $B = 489\,\text{mm}$, mean rear wheel radius $r_r = 117.5\,\text{mm}$, grousser pitch angle $\alpha_g = 45°$, and distance from axle to axle $l_{rov} = 522\,mm$. Applying this values to the above mentioned equations yields a higher rotation speed of the rear motors by factor $F \approx 1.5$ for driving straight and a factor of $F_{sts} \approx 3.1$ for side-to-side steering maneuvers.

Following smooth trajectories is possible by continuous steering. Continuous steering maneuvers are achieved by applying different nominal rotation speeds to the left and right sided wheels. The resulting wheel trajectories of each rover side are drawn in Figure 4(b). The factor ΔF_{cont} representing the nominal wheel speed ratio for the left and right side is then calculated by equation 10.

$$\Delta F_{cont} = \frac{C_o}{C_i} = \frac{r_o}{r_i} \tag{10}$$

C_o and C_i are representing the circumferences of the outer and inner trajectories, which are thus depended on the outer and inner turning radius given as $r_o = r_{turn} + \frac{B}{2}$ and $r_i = r_{turn} - \frac{B}{2}$.

3.2 Wheel development and evaluation

The side-to-side steering concept using helical rear wheels was proven by a comparison of normal skid steering with the rotational point centered between front and rear axis and a side-to-side steering set-up with the point of rotation on the front axis. The test was conducted with the Coyote I rover using cylindrical helical wheels. The track characteristics of both set-ups are shown in Figure 5. The shift of the point of rotation can clearly be identified as well as the reduced soil disturbance of the hybrid legged-wheels.

During the cylindrical helical wheel tests, two main shortcomings were observed. First, a major soil blister accumulates in front of the wheel and second, soil accumulates within the wheel rim. Following these observations a new improved design was developed. This wheel follows a spherical shape in order to reduce the soil blister at sideways motions. The wheel rim is designed with cut-outs allowing the soil to float out during rotation. The changed shape of the wheel shows a good improvement in terms of a smooth movement over soft soil. A comparison of the soil blister is highlighted in Figure 6.

Additional experiments were conducted to analyze the point turn performance of different wheel set-ups. The following five wheels were compared performance wise: (1) Cylindrical helical wheels (cf. Figure 6(a)) ($r = 100\,\text{mm}$, $w = 70\,\text{mm}$, $\alpha_g = 45°$), (2) Spherical helical wheels (cf. Figure 6(b)) ($r = 125\,\text{mm}$, $w = 120\,\text{mm}$, $\alpha_g = 45°$), (3) Asguard hybrid legged-wheels (cf. Figure 7(a)) ($r_f = 185\,\text{mm}$, $w = 27\,\text{mm}$), (4) CESAR-like hybrid legged-wheels (cf. Figure 1) ($r_f = 185\,\text{mm}$,

(a) Point turn by skid steering

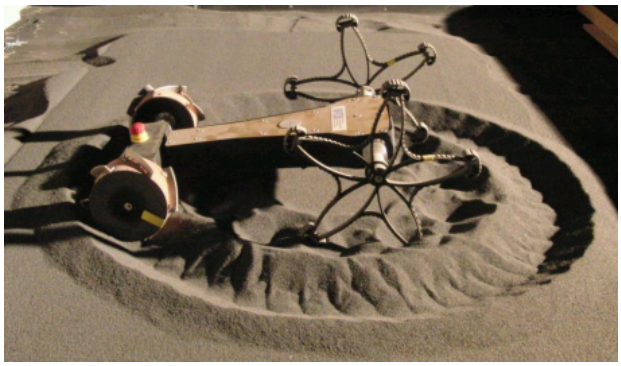

(b) Point turn by side-to-side steering

Figure 5. Point turn steering comparison

(a) Cylindrical helical wheels

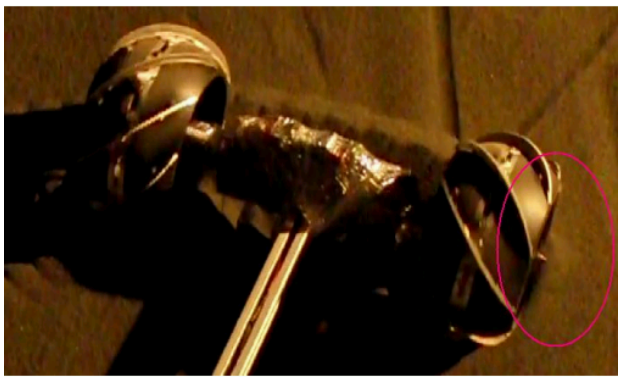

(b) Spherical helical wheels

Figure 6. Helical wheel soil blister comparison

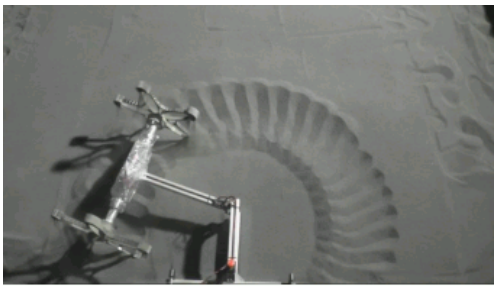

(a) Asguard wheels

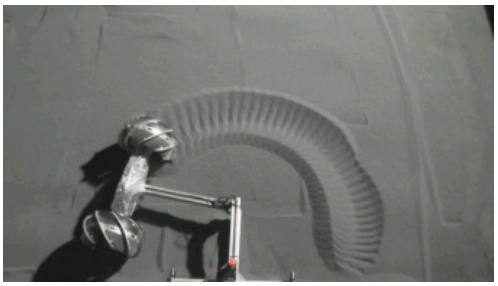

(b) Spherical helical wheels

(c) Reference wheels

Figure 7. Point turn test bench wheel track comparison and performance analysis

$w = 90\,\text{mm}$) and (5) Reference rubber wheels (cf. Figure 7(c)) ($r_f = 200\,\text{mm}$, $w = 45\,\text{mm}$).

Both helical wheels perform the point turn motion very smooth with a different performance as described previously (cf. Figure 7(b)). The Asguard hybrid legged-wheel performs the point turn with heavy digging through the soil (cf. Figure 7(a)). The difference in performance of the spherical helical wheel and the Asguard wheel can be observed in the overall power consumption as well. Figure 8 shows a plot of overall power consumption for both wheel types. The CESAR-like wheel in comparison gets stuck in the soft soil due to its asymmetrical feet shape. The round reference wheel is not able to perform the point turn as well. As shown in Figure 7(c), the wheels are digging heavily into the soil until they get stuck.

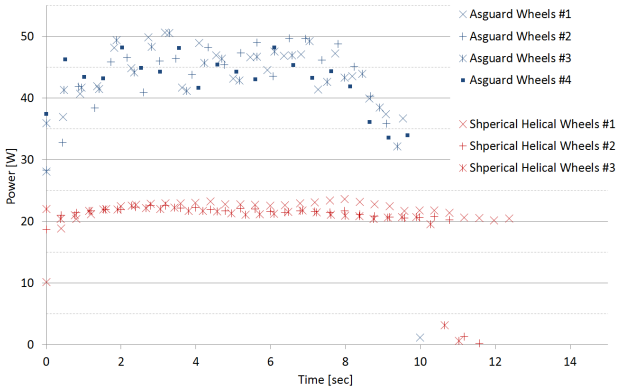

Figure 8. Point turn test bench overall power consumption

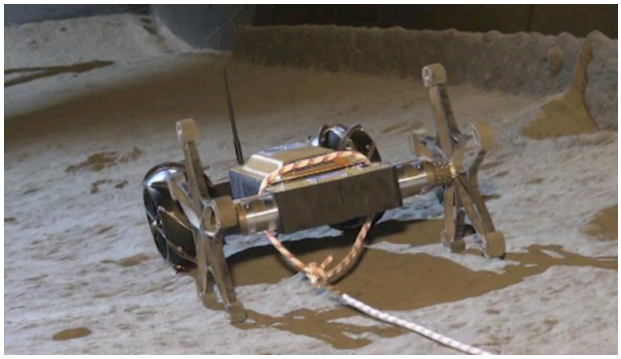

Figure 9. Coyote II driving on a 25° slope of firm soil

4 Mobility Tests

In terms of mobility the main challenge was the development of a wheel set-up able to perform on firm rough terrain as well as on very soft soils. In addition to the point turn wheel evaluation, different wheel set-ups have been tested on Coyote II. In order to perform scouting tasks for a primary rover, the scout rover needs to provide high mobility. The aim of the tests is to further evaluate the mobility performance of a four hybrid legged-wheel Asguard-like configuration and the hybrid legged-wheel plus spherical helical wheel set-up.

Asguard showed its good slope climbing abilities covering slopes of $> 25°$ in [7]. With Coyote II, as shown in Figure 9, a 25° slope climbing test was conducted. The rover performed well in upward and downward direction.

In terms of step climbing the helical wheel set-up falls short against the four hybrid legged-wheel configuration which can cover steps of $\geq 310\,\text{mm}$. With helical rear wheels the rover is able to overcome a step of 100 mm, while it is expected that the wheels can cover steps of up to 125 mm due to the wheel radius. It might even be possible to climb over higher steps in case the front wheels have

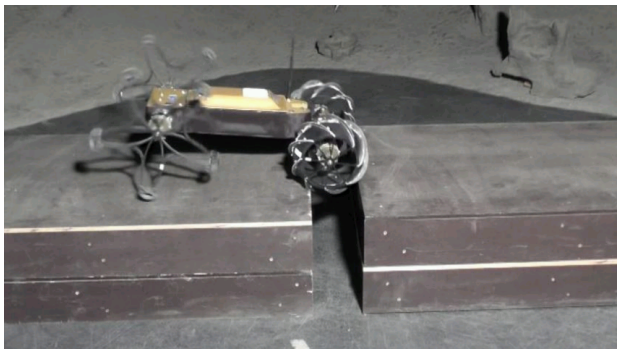

(a) 200 mm crevasse

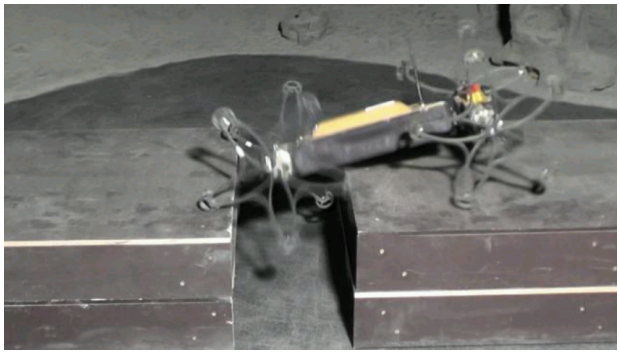

(b) 300 mm crevasse

Figure 10. Crevasse test with a helical rear wheel set-up and a four hybrid legged-wheel configuration

sufficient grip to pull the rear wheels over the obstacle. This was however, not covered during testing.

Similar to step climbing capabilities, the performance for overcoming crevasses is dependent on the wheel radius. While the hybrid legged-wheels succeed in driving over a 300 mm wide canyon, the helical wheels successfully crossed a 200 mm crevasse while they are theoretically able to cross up to 250 mm (cf. Figure 10). An observed drawback of the hybrid legged-wheels is that the legs can potentially get stuck within the crevasse.

The static stability of the systems was tested in four angles measured against the inclination: 0°, 45°, 90°, 180°. Therefore, a static stability of $\geq 45°$ is reached for both configurations in all directions.

In addition to the laboratory tests, the Coyote II rover was tested in different real environments covering a wide range of different obstacles. Overall it is expected to reach a higher mobility with a four hybrid legged-wheel set-up due to its very good climbing abilities. However, the hybrid legged-wheel, helical wheel configuration shows a good mobility as well and outperforms the first set-up in terms of steering, especially in producing less disturbances in soft soils. The helical rear wheels show the additional effect of smoothing the body movement during driving. Following the specific needs of the scout rover within the FASTER scenario, it is proposed to equip the scout rover with hybrid legged-wheels in the front and spherical helical wheels in the rear. The corresponding scout rover locomotion set-up is shown in Figure 11.

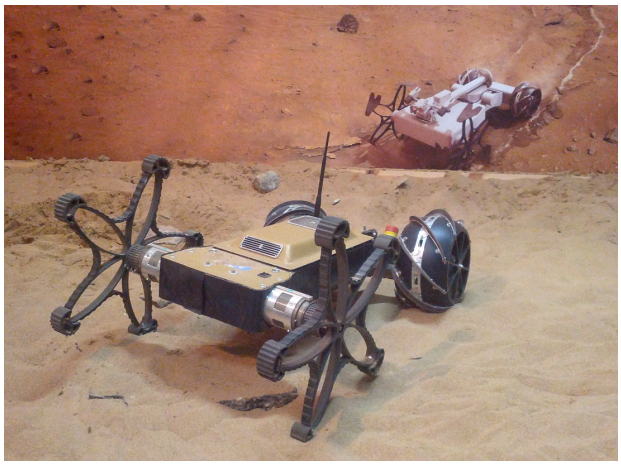

Figure 11. Coyote II in its proposed locomotion configuration operating in different soft soil types mixed with rocks

5 Scout Rover Operations

While a decentralized multi-rover system allows greater redundancy and flexibility, the FASTER concept envisages the primary rover as the mission critical component carrying the majority of scientific and operations payloads with the scout rover serving as a semi-autonomous remote sensor platform. The primary rover is designed to execute most deliberative and high level functions, thus limiting the scout rover's autonomy and consequently the required computational power and power consumption.

The overall system, comprising the two rovers, is conceived to move over long distances using the best of many waypoint based paths identified by ground operators (where the set of paths is encoded as a traverse graph). While selecting the best path to the target location is a task of variable complexity, it is mostly based on standard graph search methods. It is the coordination of the rovers as they travel from waypoint to waypoint, using a scheme inspired by the Motion-to-Goal and Boundary-Following concepts as descried in [6, 11], that is of interest. During normal waypoint traversal operations, the scout rover will travel within a distance of ~4 m ahead of the primary rover performing trafficability measurements using

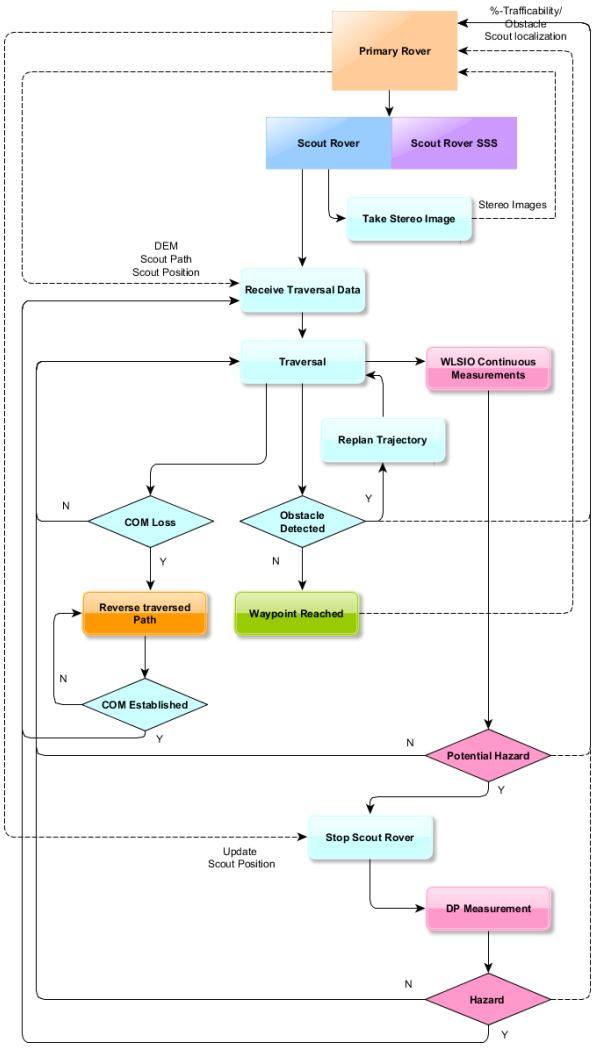

Figure 12. Schematic of normal scout rover operations

its soil sensor payloads (WLSIO[1] and DP[2]) as described in [4]. In this context, the scout rover needs to be able to travel along a predefined path on a given local digital elevation model (DEM), performing hazard avoidance and self-localization.

Each such traversal sequence starts with both rovers close to each other. The primary rover then creates a local elevation map, based on stereo images taken by both rovers. The scout rover stereo images are merged into the map to cover blind spots caused by the scout rover. Additionally, the images and/or data from the primary rover need to be filtered to ensure that the scout rover is not included as part of the elevation map. Using the created

[1]Wheel Leg Soil Interaction Observation System
[2]Dynamic Plate

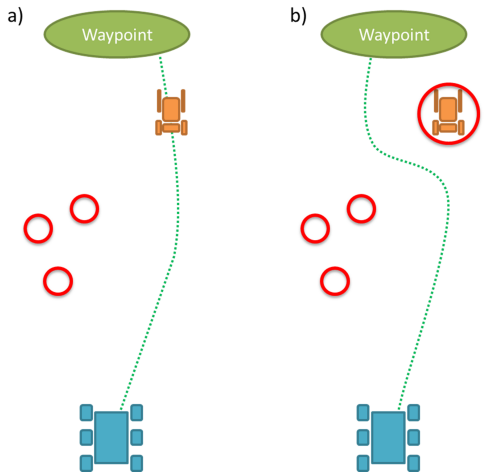

Figure 13. Dynamic path planning approach (planned path as green dots, obstacles as red circles); a) scout traversing a planned path, b) new path after newly discovered terrain hazard

map the primary rover plans local paths for both rovers, and transmits the corresponding path and elevation map to the scout. First the scout rover and then the primary rover move along the planned path, and such short traverses are repeated till the next waypoint is reached. The general schematic of the scout rover operation is shown in the action flow diagram in Figure 12.

In certain cases of hazard detection during traversal, as well as some emergency scenarios like communication loss, the scout rover needs to return to the primary rover using the known map and path. If a *NO-GO* area is detected by the scout rover's soil sensor system the scout awaits new traversal data from the primary rover. This can either mean to return to the primary rover for a new traverse sequence or to receive a locally replanned path from a dynamic path planner (on the primary rover) as illustrated in Figure 13.

The proposed navigation stack for the scout rover is illustrated in Figure 14. It makes use of an odometry based trajectory follower. Additionally, a local planner is proposed to be implemented to the navigation stack allowing to create transient maps of the close surrounding of the scout rover. The local planner is intended to use the Vfh* method [10], allowing obstacle avoidance by providing short trajectories in a certain direction and optimizing the required steering movements.

As the scout rover serves as a mobile hazard detector, knowing its location relative to the primary rover accurately is extremely important to appropriately localize and avoid the detected hazards. While the scout rover maintains an odometry based pose estimate, the primary rover

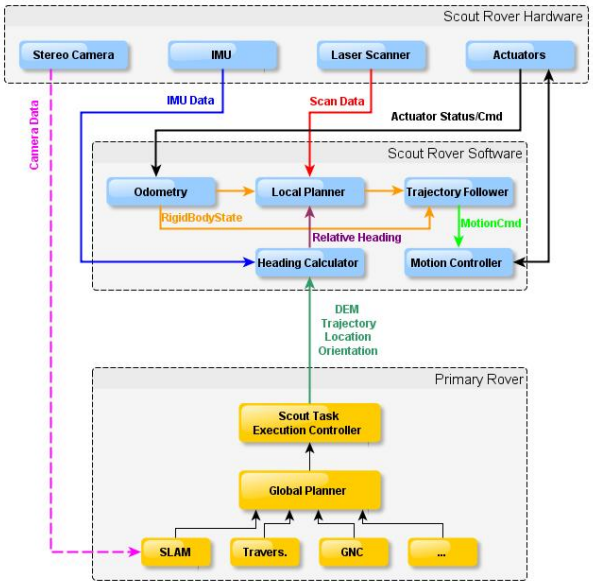

Figure 14. Proposed architecture of the scout rover navigation stack for dual rover operations

additionally calculates the relative position of the scout to correct errors and large drift. For this purpose a marker based approach using the primary rover's stereo camera bench is implemented on the primary rover.

6 Conclusion and Outlook

Within the previous sections the terrestrial test platform Coyote II is presented. The rover is equipped with a novel locomotion system applying hybrid legged-wheels in the front and spherical helical wheels in the rear, allowing side-to-side steering maneuvers. The chosen locomotion set-up yields high versatility and mobility for rough terrain as well as for very soft soils and is proven in various laboratory and real environment tests. The rover is intended for scouting purposes, paired up with a primary rover. The scout rover operation within a dual rover team is addressed in order to increase the safety of autonomous long term explorations as proposed by the FASTER project.

The dual rover configuration will be further tested in simulation and applied to real robotic systems. Therefore, the presented micro rover will be adapted to carry additional soil sensor payloads. For overall software and autonomy testing, the BRIDGET locomotion testbed [3] from Astrium Ltd. will be used as primary rover.

Acknowledgment

The work presented is part of the Forward Acquisition of Soil and Terrain Data for Exploration Rover (FASTER)-project. The project is funded by the EU FP7 program under grand agreement no. 284419.

References

[1] S. Bartsch et al. "SpaceClimber: Development of a Six-Legged Climbing Robot for Space Exploration". In: *Proc. of the joint Conf. of ISR 2010 (41st Int. Symp. on Robotics) and ROBOTIK 2010 (6th German Conf. on Robotics)*. VDE, 2010.

[2] M. Eich, F. Grimminger, and F. Kirchner. "A Versatile Stair-Climbing Robot for Search and Rescue Applications". In: *Proc. of the IEEE, Int. Workshop on Safty, Security and Rescue Robotics*. Sendai, Japan, 2008.

[3] C. G-Y. Lee et al. "Design and Manufacture of a Full Size Breadboard Exomars Rover Chassis". In: *Proc. of the 9th Symp. on Advanced Space Technologies in Robotics and Automation (ASTRA-2006)*. Noordwijk, the Netherlands, 2006.

[4] W.A. Lewinger et al. "Multi-Level Soil Sensing Systems to Identify Safe Trafficability Areas for Extra-Planetary Rovers". In: *Proc. of the 12th Symp. on Advanced Space Technologies in Robotics and Automation (ASTRA-2013)*. Noordwijk, the Netherlands, 2013.

[5] Y. Nevatia et al. "Improved Traversal for Planetary Rovers through Forward Acquisition of Terrain Trafficability". In: *Proc. of IEEE Int. Conf. on Robotics and Automation (ICRA-2013), Planetary Rovers Workshop*. Karlsruhe, Germany, 2013.

[6] Y. Nevatia et al. "Safe Long-Range Travel for Planetary Rovers Through Forward Sensing". In: *Proc. of the 12th Symp. on Advanced Space Technologies in Robotics and Automation (ASTRA-2013)*. Noordwijk, the Netherlands, 2013.

[7] DFKI RIC. *Asguard v2: Field Trip June 2008*. 2008. URL: `http://robotik.dfki-bremen.de/de/forschung/robotersysteme/asguard-ii.html`.

[8] J. Schwendner et al. "CESAR: A Lunar Crater Exploration and Sample Return Robot". In: *Proc. of the IEEE/RSJ Int. Conf. on Intelligent Robots and Systems*. 2009.

[9] R.U. Sonsalla et al. "Concept Study for the FASTER Micro Scout Rover". In: *Proc. of the 12th Symp. on Advanced Space Technologies in Robotics and Automation (ASTRA-2013)*. Noordwijk, the Netherlands, 2013.

[10] I. Ulrich and J. Borenstein. "VFH*: local obstacle avoidance with look-ahead verification". In: *Proc. of the IEEE Int. Conf. on Robotics and Automation - ICRA'00*. San Francisco, CA, 2000.

[11] R. Volpe et al. "Enhanced Mars Rover Navigation Techniques". In: *Proc. of the IEEE Int. Conf. on Robotics and Automation (ICRA '00)*. San Francisco, CA, 2000.